Generation of Complex Source Point Expansions from Radiation Integrals

Enrica Martini and Stefano Maci*

(*Invited Paper*)

Abstract—This paper discusses methods for expanding fields radiated by arbitrary sources enclosed by a certain minimum sphere in terms of Complex Source Point (CSP) beams. Two different approaches are reviewed; the first one is based on a spectral radiation integral, where the Fourier-spectrum is obtained by far field matching. The second approach consists of two steps: first, the equivalence principle is applied to a sphere enclosing the real sources, and a continuous equivalent electric current distribution is obtained in terms of spherical waves; then, the continuous current is extended to complex space and its SW components are properly filtered and sampled to generate the discrete set of CSPs. In both cases, the final result is a compact finite series representation with a number of terms that matches the degrees of freedom of arbitrary radiated fields; it is particularly efficient when the fields are highly directional and the observation domain is limited to a given angular sector. The fact that the CSPs rigorously respect Maxwell's equations ensures the validity of the expansion from near to far zone and allows one to incorporate the CSP representation in a generalized admittance matrix formalism for the analysis of complex problems.

1. INTRODUCTION

In many electromagnetic problems, beam expansions represent a useful means to efficiently analyze interactions between parts of the system. Indeed, thanks to their angular selectivity, only a limited number of beams significantly contribute to the field in a given angular observation region. Generally speaking, a beam is a wave object whose amplitude is confined to a region of space around a certain direction of propagation, i.e., the direction along which it exhibits a phase progression. A beam may be an exact solution of the wave equation, an approximate solution of the wave equation, or a solution of an approximation of the wave equation. Different types of beams have been introduced in the literature, the most popular of which are listed below

- Gaussian Beams (GBs).
- Higher order Gaussian-Laguerre Beams (GLBs).
- Higher order Gaussian-Hermite Beams (GHBs).
- Bessel Beams (BBs).
- Gaussian-ray basis functions (GRBFs).
- Complex Conical Beams (CCBs).
- Complex Source Points (CSPs).

GBs [1, 2] are the most commonly used, especially for representing field radiated from conical corrugated horns and from reflectors. A GB satisfies Maxwell's equations only in the paraxial region, namely close to the axis of propagation. GLBs or GHBs [3–5] deal with expansions around a preferred axis of propagation with the higher order terms representing the off-axis variations. They have the advantage of constituting an orthogonal set, and they are often used as basis for a mode matching technique. GLBs and GHBs are more suitable for describing rectangular and circular apertures, respectively. Their descriptive capability relaxes but does not remove the restriction to satisfy Maxwell's equations only in the paraxial region; this produces slow convergence in describing far out-of axis lobes.

In Fourier Optics, the field is often represented by a discrete spectrum of BBs [6]. BBs are quite similar to GHBs, but unlike the latter they do not diffract as they propagate, thus exhibiting a non-physical behavior in far region. However, they are useful in near field and laser beam representations.

In contrast with the previously described GB plus higher order beams, which can provide a *global* description of the field radiated by an aperture, Gabor-type (or phase-space) expansions [7–10] provide a *local* far field (aperture field spectrum) description. The field is expanded using a lattice of beams that emerge from a set of points in the aperture plane and propagate from each point in a lattice of directions. The beam amplitudes are determined by the local radiation properties (local spectrum) of the aperture near the lattice spectral points. This beam representation can be viewed as a "local" expansion of the aperture field spectrum. It is seen that, for off-axis observation, the localized nature of the spectral elements implies more rapid convergence than with global expansions [11]. In the Gabor-based Gaussian beam expansion, the basis set is complete; this poses a restriction on the choice of the spatial and spectral resolutions. The Gabor-frame scheme in [7, 8] (termed there "windowed Fourier transform frame") relaxes this restriction by using overcomplete sets of GBs, thus enabling the user to choose the spatial and spectral resolutions that best fit the local properties of the source distribution. Furthermore, the flexibility gained by using the overcomplete frame expansion allows for an efficient representation of ultrawide band fields [9, 10].

GRBFs [12, 13] are used to locally match the far field as in the Gabor expansion; however, they have more degrees of freedom, obtained by introducing an empirical extra parameter to a conventional Gaussian beam, in order to manually control beam width at a given distance from the source.

The CCBs introduced in [14] present a selective concentration of energy around the surface of a cone, and their representation rigorously satisfies the wave equation. An aperture field representation in terms of these beams is generated in a natural way starting from the spectral-domain radiation integral. This is done by first expanding the electric field spectrum in a Fourier series and next approximating the obtained Fourier series coefficients through a sum of complex exponentials using the generalized pencil-of-function (GPOF) method [15], which leads to a final sum of conical beams.

An alternative to the global Gabor expansion is represented by the CSP expansion [16–19]. A CSP differs from a GB only far from its axis. While GB is an approximate paraxial solution of the wave equation, the CSP is an exact solution of the wave equation, except at a circle of singularities. The most popular use of CSPs is concerned with expansion of space domain Green's functions of layered dielectric media [20, 21]. To this end, the spectral Green's function is represented in terms of exponentials by using the GPOF method, thus leading to the CSP expansion by using the well-known Sommerfeld integral. A similar technique is used to regularize the Kernel of 3D integral equations [22].

In this paper, we focus our attention on CSP beams. Two different approaches are discussed, generalizing works already published by the authors and revisiting them in a unified approach, while introducing new results. The first approach is based on a spectral version of the radiation integral, where the spectrum is reconstructed by far field matching. The second approach consists in the use of the equivalence principle applied to a sphere enclosing the real sources; a continuous equivalent current distribution is obtained in terms of spherical waves (SWs) and then extended to complex space. Finally, the SW components are properly filtered and sampled to generate the discrete set of CSPs. Both approaches are minimally redundant, namely satisfy the degrees of freedom of the field described in the next section.

2. DEGREES OF FREEDOM OF THE FIELD

The definition of a non-redundant field representation is strictly related to the concept of degrees of freedom (DoF) of the field [23]. The DoF of the field radiated by an arbitrary source contained in a surface S in a given observation domain can be defined as the minimum number of independent coefficients of any type of discrete field expansion that allows for an accurate field description in that observation domain. A general way to determine the DoF relies on the use of a singular value decomposition (SVD) of the radiation operator which maps the currents on the source boundary S onto the field radiated in the observation domain. The SVD identifies a set of orthogonal functions (also referred to as "modes") to expand the radiated field and a set of orthogonal modes, and relevant singular values, to expand the currents. Current modes associated with vanishingly small singular values only contribute to the evanescent field in the neighboring of the sources and contribute negligibly to the radiated field. Hence, in presence of a noise, they are not observable at a certain distance from the sources. For this reason, only a subset of current modes are significant for describing the non-evanescent field, and the dimension of this subset defines the number of DoF of the radiated field. There is in principle an ambiguity in the definition of the number of DoF, since it apparently depends upon an assumed dynamic range of the radiation efficiencies. However, this is not a practical issue, because, due to the fact that the radiation operator is compact, the singular values tend exponentially fast to zero when their order tends to infinity, making the identification of the DoF almost insensitive to the required precision [24, 25].

As a general rule, the number of DoF is essentially a function of the electrical size of the source distribution and, although strictly speaking it depends on the observation distance, its value stabilizes outside the reactive region of the sources. In the particular case in which the minimum surface S enclosing the sources and the observation surface S' are concentric spheres, the singular functions of the radiation operator are spherical modes, and the relevant singular values can be calculated in closed form; outside the reactive region, the number of DoF turns out to be approximately equal to $N_{DoF} = 2(kr_{\min})^2$ where k is the wave number and $r_{\min}$ is the radius of S. In this case, the spherical harmonics represent the optimal basis for the field representation. N_{DoF} also provides the minimum number of wave objects for the representation of the radiated field in the absence of any a priori knowledge of the sources enclosed by S. If, instead, the actual location of the sources inside S is known, the number of modes required for the field representation may be significantly lower than N_{DoF}. For instance, for planar source distributions the number of degrees of freedom is given by the Landau-Pollak bound [11] and ad hoc sets of functions can be defined for the field representation [8, 26–29]. When also the source distribution is known, the number of basis functions can be further reduced by a priori selecting a subset of the general basis [8] or by using field-matched wave objects [14]. However, in this latter case a different set of basis functions must be defined for each source distribution. A wave-field basis independent of the sources is indeed more important when one would like to use it in a general numerical method.

In certain cases one is interested in the field radiated only in directions belonging to a limited angular sector. For instance, this occurs when calculating the interactions between well separated groups of basis functions [30] or the interactions between two sub-domains [31]. When the observation domain is restricted to a limited solid angle Ω, the analysis of the singular values reveals that the number of DoF is reduced by a factor approximately equal to the ratio between Ω and 4π, $N_{DoF}^{\Omega} \approx 2(kr_{\min})^2[\Omega/4\pi]$. Spherical harmonics no longer represent an optimal basis for the current representation, since in general all the first N_{DoF} harmonics provide a non-negligible contribution in the angular sector Ω, due to their poor angular selectivity. The optimal basis is constituted by the N_{DoF}^{Ω} orthogonal modes associated with the dominant singular values, which are obtained as SVD-based linear combinations of the first N_{DoF} spherical harmonics. Such a basis must be constructed numerically and depends on the given observation domain Ω. When elements from the same basis must be used to represent the field in different observation domains, like in the approaches of [30, 31], a more convenient way to reduce the redundancy consists in using beams as basis functions and exploiting their angular selectivity to identify the important contributions for any given angular sector Ω.

3. COMPLEX SOURCE POINTS

Among the various kinds of beams, the CSP-beams have the advantage of being exact solutions of the wave equation and of maintaining their simple functional form in the whole space [17, 18]. A spherical wave of type $\exp(-jkR)/R$ with $R = \sqrt{(\mathbf{r} - \mathbf{r}_0) \cdot (\mathbf{r} - \mathbf{r}_0)}$ respects the wave equation also when the center of phase $\mathbf{r}_0$ is formally displaced in a complex point $\mathbf{r}_c = \mathbf{r}_0 - j\mathbf{b}$. The waveform obtained by this complex displacement is called CSP. After the analytical continuation, the complex distance R is a multivalued function which respects the radiation condition when $\mathrm{Re}(R) \geq 0$. It is found that R is equal to zero — and therefore the field is singular — on the rim of a disc of radius $b = |\mathbf{b}|$ orthogonal to $\mathbf{b}$ and centered in $\mathbf{r}_0$. In the half space $(\mathbf{r} - \mathbf{r}_0) \cdot \mathbf{b} > 0$ the CSP exhibits a behavior quite similar to a Gaussian beam propagating along $\mathbf{b}$, with waist $|\mathbf{b}|$. In particular, assume that the complex displacement is along the z axis of a Cartesian reference system ($\mathbf{b} = -jb\hat{\mathbf{z}}$ and that the phase center is at $\mathbf{r}_0 \equiv 0$. In the paraxial region (defined as $x^2 + y^2 \ll z^2 + b^2$) one has $R = \sqrt{x^2 + y^2 + (z + jb)^2} \approx z + jb + (x^2 + y^2)/(2z + 2jb)$ and therefore

$$G_0(R) = \frac{\exp(-jkR)}{4\pi R} \approx \frac{e^{kb}}{4\pi (z + jb)} e^{-jkz\left[1 + \frac{1}{2}\frac{(x^2+y^2)}{(z^2+b^2)}\right]} e^{\frac{-kb}{2}\frac{\left(x^2+y^2\right)}{(z^2+b^2)}} \tag{1}$$

which exhibits the Gaussian-beam like behavior.

The electric field of a vector CSP oriented along a unit vector $\hat{\mathbf{u}}$ can be written as

$$\mathbf{E}_{CPS}^J(\mathbf{r}) = \underline{\underline{\mathbf{G}}}_{EJ}(\mathbf{r} - \mathbf{r}_c) \cdot \hat{\mathbf{u}}; \quad \underline{\underline{\mathbf{G}}}_{EJ}(\mathbf{r}) = jk\zeta G_0(R) \left\{ \left(1 + \frac{1}{jkR} - \frac{1}{(kR)^2}\right) \hat{\mathbf{r}} \times \left(\hat{\mathbf{r}} \times \underline{\underline{\mathbf{I}}}\right) + 2\left(\frac{1}{jkR} - \frac{1}{R^2}\right) \hat{\mathbf{r}}\hat{\mathbf{r}} \right\} \tag{2}$$

$$\mathbf{E}_{CPS}^M(\mathbf{r}) = \underline{\underline{\mathbf{G}}}_{EM}(\mathbf{r} - \mathbf{r}_c) \cdot \hat{\mathbf{u}}; \quad \underline{\underline{\mathbf{G}}}_{EM}(\mathbf{r}) = -jkG_0(R) \left(1 + \frac{1}{jkR}\right) \left(\hat{\mathbf{r}} \times \underline{\underline{\mathbf{I}}}\right) \tag{3}$$

where ζ is the free-space impedance, G_0 is the scalar free-space Green's function in (1), and $\underline{\underline{\mathbf{G}}}_{EJ}$ and $\underline{\underline{\mathbf{G}}}_{EM}$ are the dyadic Green's functions for the electric and magnetic source, respectively. Furthermore, $R = \sqrt{\mathbf{r} \cdot \mathbf{r}}$, $\hat{\mathbf{r}} = \mathbf{r}/\sqrt{\mathbf{r} \cdot \mathbf{r}}$ are complex values when evaluated at $\mathbf{r} - \mathbf{r}_c = \mathbf{r} - (\mathbf{r}_0 - j\mathbf{b})$. The fields in (2)–(3) rigorously satisfy free-space Maxwell's equations in any space point, except at the branch line $(\mathbf{r} - \mathbf{r}_c) \cdot (\mathbf{r} - \mathbf{r}_c) = 0$. The relevant 3D Fourier spectrum can be written as

$$\left\{ \begin{matrix} \underline{\underline{\mathbf{G}}}_{EJ}(\mathbf{r} - \mathbf{r}_c) \\ \underline{\underline{\mathbf{G}}}_{EM}(\mathbf{r} - \mathbf{r}_c) \end{matrix} \right\} = j \left(\tfrac{1}{2\pi}\right)^3 \int\limits_{-\infty}^{+\infty} \int\limits_{-\infty}^{+\infty} \int\limits_{-\infty}^{+\infty} \left\{ \begin{matrix} \frac{\zeta}{k}\mathbf{k} \times \left(\mathbf{k} \times \underline{\underline{\mathbf{I}}}\right) \\ -\mathbf{k} \times \underline{\underline{\mathbf{I}}} \end{matrix} \right\} \frac{\exp\left(-j\mathbf{k} \cdot (\mathbf{r} - \mathbf{r}_c)\right)}{\mathbf{k} \cdot \mathbf{k} - k^2} W(\mathbf{k}) d\mathbf{k}^3 \tag{4}$$

where $\mathbf{k} \equiv (k_x, k_y, k_z)$, $d\mathbf{k}^3 = dk_x dk_y dk_z$ and $W(\mathbf{k})$ is an arbitrary differentiable windowing function of $\mathbf{k}$, which is unity on the sphere $\mathbf{k} \cdot \mathbf{k} = k^2$ and decays exponentially faster than $\exp(-b(\mathbf{k} \cdot \mathbf{k} - k^2))$ for $|\mathbf{k}| \to \infty$. The spherical surface $\mathbf{k} \cdot \mathbf{k} = k^2$ is denoted hereinafter as "spectral visible sphere" (SVS). We note that the exact values $W(\mathbf{k})$ assumes outside the SVS do not affect the final result, since the Devaney-Wolf theorem in [34] ensures that the value of the integral is defined only by the values the integrand assumes on the SVS. By applying the Jordan Lemma, indeed, the integral in (4) can be reduced to a $W(\mathbf{k})$ — independent double integral at a pole $\mathbf{k} \cdot \mathbf{k} = k^2$. However, we prefer here maintaining the triple integral form in (4) for reasons that are clarified next.

CSPs have the capability of constructing an expansion of a given electromagnetic field with moderate redundancy, namely almost matching the degrees of freedom of the field. A complex source representation based on complex equivalent principle for only scalar fields was first proposed in [19]. In [32], an exact CSP expansion for arbitrary scalar fields was presented, where the beams are launched from a single point in space and their coefficients are determined on the basis of the field radiated on a sphere in real space. More recently, alternative formulations have been provided in [30, 33] where the beams are launched from a sphere enclosing the real sources. A first formulation uses both electric and magnetic equivalent sources, whose weights are related, through the equivalence theorem, to the analytic continuation in complex space of the field to be represented. A second formulation uses only electric CSP and determines their coefficients by solving a linear system. The latter is constructed by matching the field to be expanded with the CSP beam expansion at a proper set of points on a spherical

test surface. This second approach allows for the minimization of the number of CSP beams, but it requires the solution of a linear system for the determination of the expansion coefficients. On the other hand, the first approach provides a closed form expression of the beam weights, but it requires a larger number of beams due to the high sampling density needed to accurately discretize the radiation integral. Further redundancy is related to the use of both electric and magnetic type sources, since the two associated sets of beams are not independent. If the equivalence surface is taken close to the sources, the equivalent currents exhibit rapid variations related to the reactive part of the field. The reactive fields are not observable at a few wavelengths distance from the sources; however, considering a larger equivalence surface would not resolve the problem, since it would lead to faster variations of the dyadic Green's function appearing in the integrand of the radiation integral. In the following, the previous approach will be revised with the objective of minimizing the redundancy. Furthermore, in the next section, a rigorous spectral domain formulation is presented to rigorously justify the far field matching approach in [30, 31].

4. CSP-GENERATION BY SPECTRAL SAMPLING

Let us consider an arbitrary set of currents $\mathbf{j}(\mathbf{r})$, $\mathbf{m}(\mathbf{r})$ enclosed by a minimum sphere of radius $r_{\min}$. The radiation integral in any point of space outside this minimum sphere can be represented by a 3D Fourier-type spectral radiation integral

$$\mathbf{E}(\mathbf{r}) = \frac{1}{8\pi^3} \int\limits_{-\infty}^{+\infty} \int\limits_{-\infty}^{+\infty} \int\limits_{-\infty}^{+\infty} \mathbf{F}(\mathbf{k}) \frac{\exp(-j\mathbf{k}\cdot\mathbf{r})}{\mathbf{k}\cdot\mathbf{k} - k^2} d\mathbf{k}^3 \tag{5}$$

where $F(\mathbf{k}) = j\frac{\zeta}{k}\mathbf{k} \times (\mathbf{k} \times \mathbf{J}(\mathbf{k})) - j\mathbf{k} \times \mathbf{M}(\mathbf{k})$ and $[\mathbf{J}(\mathbf{k}), \mathbf{M}(\mathbf{k})]$ are the spectra of $[\mathbf{j}(\mathbf{r}), \mathbf{m}(\mathbf{r})]$ [34]. An asymptotic evaluation of the integral in (5) at a large distance r from the origin is obtained by the residue evaluation of one of the integrals at $\mathbf{k}$ such that $\mathbf{k} \cdot \mathbf{k} = k^2$, followed by the stationary phase contribution at $\mathbf{k} = k\hat{\mathbf{r}}$ where $\hat{\mathbf{r}}$ is the radial space unit vector, i.e.,

$$\mathbf{E}(\mathbf{r}) \approx [\mathbf{F}(\mathbf{k})]_{\mathbf{k}=k\hat{\mathbf{r}}} \frac{\exp(-jkr)}{4\pi r} \quad r > r_{far} = 8r_0^2/\lambda \tag{6}$$

To fit the field at any space point in the spectral representation (5), we construct a lattice of spectral directions $\hat{\mathbf{k}}_p$, $p = 1, 2, \ldots, P$, where P matches $N_{DoF}/2 = (kr_{\min})^2$ with a small redundancy (the factor 2 is because the two polarizations can be matched using a single point),

$$P \approx (kr_{\min}\eta)^2 \tag{7}$$

where P is the integer that best approximates the right hand side. In (7), η is a redundancy factor typically ranging from 1 to 1.3. The intersections of the directions aligned with $\hat{\mathbf{k}}_p$ with the SVS, namely the points $k\hat{\mathbf{k}}_p$, constitute the vertexes of triangles of sub-areas approximately equal each other and therefore equal to $4\pi k^2/P = 4\pi/(\eta r_{\min})^2$ (Figure 1(a)). Many algorithms can be applied to maintain the areas of the triangles as uniform as possible, for instance the quadrature rule in [35]. The average side Δk of each triangle is obtained by assuming that all the triangles are equilateral; this leads to $\Delta k \approx \sqrt{8\pi/\sqrt{3}}/(\eta r_0) = 5.39/(\eta r_{\min})$; the angle between two contiguous unit vectors $\hat{\mathbf{k}}_p$ is therefore $\Delta\alpha = \Delta k/k = \lambda/(\eta r_{\min}1.17)$.

To fit the spectrum we use the spectral basis

$$\mathbf{j}_p^{(\varphi)}(\mathbf{k}) = j\frac{\zeta}{k}\mathbf{k} \times (\mathbf{k} \times \hat{\boldsymbol{\varphi}}_p) \exp\left(-j\mathbf{k}\cdot\mathbf{r}_p^{(c)}\right); \quad \mathbf{j}_p^{(\theta)}(\mathbf{k}) = j\frac{\zeta}{k}\mathbf{k} \times \left(\mathbf{k} \times \hat{\theta}_p\right) \exp\left(-j\mathbf{k}\cdot\mathbf{r}_p^{(c)}\right) \tag{8}$$

where $\hat{\boldsymbol{\varphi}}_p = (\hat{\mathbf{z}} \times \hat{\mathbf{k}}_p)/|\hat{\mathbf{z}} \times \hat{\mathbf{k}}_p|$; $\hat{\theta}_p = \hat{\boldsymbol{\varphi}}_p \times \hat{\mathbf{k}}_p$, $\mathbf{r}_p^{(c)} = \hat{\mathbf{k}}_p(r_0 - jb)$ and $r_0 \leq r_{\min}$. It is evident from (4) that (8) are the 3D Fourier spectra of an electric CSPs oriented along $\hat{\boldsymbol{\varphi}}_p$ and $\hat{\theta}_p$. Each spectral basis function in (8) is spectrally selective, since it is attenuated at contiguous nodes of the spectral lattice by a factor $\exp(-kb(\Delta\alpha)^2)$ (see Figure 1(a)). Therefore, the significant part of the amplitude spectra in (8) extends in a region of radius inversely proportional to kb around each spectral point $k\hat{\mathbf{k}}_p$ (Figure 1(a)).

(a)   (b)
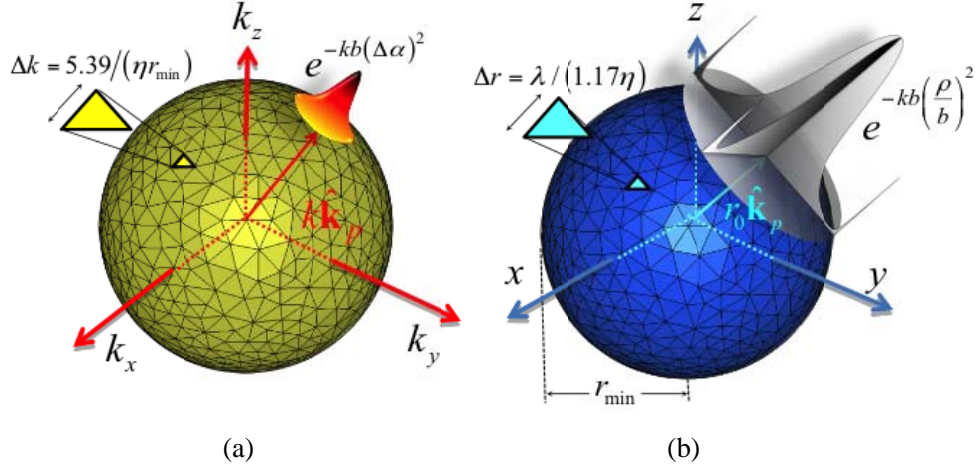
Figure 1. Spectral visible sphere (SVS) meshed in triangles with average inter-node distance $\Delta k = 5.39/(\eta r_{\min})$; the spectral CSP basis is spectrally selective for large values of b. (b) Minimum sphere enclosing the source meshed with inter-node distance $\lambda/(1.17\eta)$ and picture of a beam in the near region for a value of b comparable with the radius of the minimum sphere.

We expand the spectral function $\mathbf{F}(\mathbf{k})$ in terms of the spectral basis in (8)

$$\mathbf{F}\left(\mathbf{k}\right) = \sum_{p=1}^{P} i_p^{(\theta)}\mathbf{j}_p^{(\theta)}\left(\mathbf{k}\right) + i_p^{(\varphi)}\mathbf{j}_p^{(\varphi)}\left(\mathbf{k}\right) \tag{9}$$

where $i_p^{(\theta)}$ and $i_p^{(\varphi)}$ are unknown coefficients. Insertion of (9) in (5) with the use of (4) leads to

$$\mathbf{E}\left(\mathbf{r}\right) = \sum_{p=1}^{P} \underline{\underline{\mathbf{G}}}_{EJ}\left(\mathbf{r} - \mathbf{r}_p^{(c)}\right) \cdot \left(i_p^{(\theta)}\hat{\boldsymbol{\theta}}_p + i_p^{(\varphi)}\hat{\boldsymbol{\varphi}}_p\right) \tag{10}$$

where $\underline{\underline{\mathbf{G}}}_{EJ}$ is defined in (2). The above equation represents an expansion of CSP-beams with phase centers at the space points $\hat{\mathbf{k}}_p r_0 = \mathbf{r}_p$, emanating radially in a lattice of directions $\hat{\mathbf{k}}_p$. This lattice segments the minimum sphere in triangles of average side $r_{\min}\Delta\alpha = \lambda/(\eta 1.17)$. Each beam has an aperture branch-disc of radius equal to b orthogonal to $\hat{\mathbf{k}}_p$ (Figure 1(b)). Therefore b large, while implying an angular selectivity in the far region, does not ensure selectivity in the near region. On the contrary, b small implies weak angular (spectral) selectivity, but it ensures a better description of the field variation close to the minimum sphere.

The expansion in (9) can be constructed by matching directly the far field (which means matching the spectrum over the SVS) in a lattice of directions $\hat{\mathbf{k}}_q$ with $q = 1, 2, \ldots, P$ coincident with the spectral sampling

$$\mathbf{E}\left(r\hat{\mathbf{k}}_q\right) 4\pi r \exp(jkr)\Big]_{r>r_{far}} = \mathbf{F}\left(k\hat{\mathbf{k}}_q\right) = \sum_{p=1}^{P} i_p^{(\theta)}\mathbf{j}_p^{(\theta)}\left(k\hat{\mathbf{k}}_q\right) + i_p^{(\varphi)}\mathbf{j}_p^{(\varphi)}\left(k\hat{\mathbf{k}}_q\right) \quad q = 1, 2, \ldots, P \tag{11}$$

The above is a $\eta^2 N_{dof} \times \eta^2 N_{dof}$ linear system in the unknown coefficients $i_p^{(\theta)}$, $i_p^{(\varphi)}$. We notice that (11) requires only the knowledge of the far field pattern samples, while, once the coefficients have been calculated, (9) is valid from the far-field region up to a few fractions of wavelengths from the surface of the minimum sphere. Thus, the above formulation is a way to reconstruct the near zone from the far zone field. The interesting aspect in (11) is that one can match only an angular region of the far field pattern, solving for a reduced number of unknowns and matching the degrees of freedom $N_{DoF}^{\Omega} = N_{DoF}\Omega/4\pi$, where Ω is the solid angular region of interest.
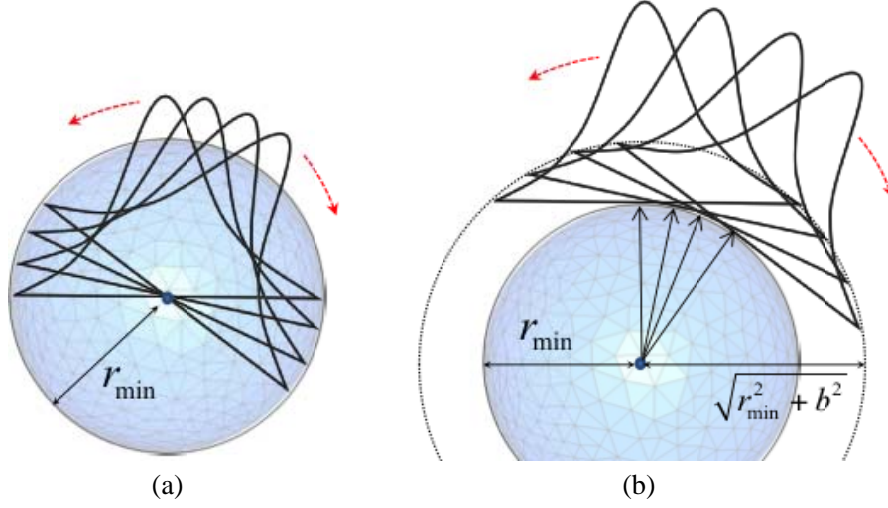
Figure 2. Space representation of field distribution at the branch-disc of CSP's with (a) $r_0 = 0$, $b = r_{\min}$ and (b) $r_0 = r_{\min}$, $b = r_{\min}$. In both cases singularities at the rim of the branch-discs are not depicted.

In the procedure described above we have not discussed the choice of b and r_0. In order to visualize how the choice of this two parameters may affect the near field accuracy, let us focus the attention on two cases: $r_0 = 0$, $b = r_{\min}$, and $r_0 = r_{\min}$, $b = r_{\min}$ (Figure 2). In both cases, the beams are spectrally selective. The beam expansion in (10) is affected by the fact that the p-indexed CSP exhibits a branch cut on a flat disc D_p of radius b, orthogonal to $\hat{\mathbf{k}}_p$ and centered at the phase center of the CSP. On the two sides of the disc, the CSP field exhibits a jump discontinuity and it is singular at the rim ∂D_p of the disc. In the case $r_0 = 0$, $b = r_{\min}$ (Figure 2(a)) all D_p are inside the minimum sphere, with rim ∂D_p on its surface. Therefore, no space point outside the minimum sphere is affected by singularity. In the second case, $r_0 = r_{\min}$, $b = r_{\min}$ (Figure 2(b)), ∂D_p are tangent to the minimum sphere, and therefore the expansion in (10) is Maxwellian only outside the sphere $r = \sqrt{r_{\min}^2 + b^2}$ while within the same sphere it may exhibit singularities. In this case, the field inside the minimum sphere is almost zero.

The far field matching can also be performed by using a redundancy of spectral samples, namely $q = 1, \ldots, Q$ with $Q > P$. This is useful to improve the condition number of the system matrix. The system in (11) can be cast in matrix form $[\mathbf{Z}][\mathbf{I}] = [\mathbf{F}]$ where $[\mathbf{Z}] = \{\mathbf{j}_p^{(\theta)}(k\hat{\mathbf{k}}_q), \mathbf{j}_p^{(\varphi)}(k\hat{\mathbf{k}}_q)\}_{\substack{p=1,P \\ q=1,Q}}$, $[\mathbf{I}] = \{i_p^{(\theta)}, i_p^{(\varphi)}\}_{p=1,P}$ and $[\mathbf{F}] = \{\mathbf{F}(k\hat{\mathbf{k}}_q), \mathbf{F}(k\hat{\mathbf{k}}_q)\}_{q=1,Q}$. This leads to a rectangular system, whose solution can be achieved on the basis of the singular value decomposition (SVD). SVD allows to factorize $[\mathbf{Z}]$ in the form $[\mathbf{Z}] = [\mathbf{U}][\mathbf{D}][\mathbf{V}]^H$ where the superscript H denotes Hermitian conjugation, $[\mathbf{U}]$ and $[\mathbf{V}]$ are unitary matrices of dimensions $2Q \times 2Q$ and $2P \times 2P$, respectively, and $[\mathbf{D}]$ is a $2Q \times 2P$ matrix whose entries are zero apart from the diagonal elements λ_j (singular values of $[\mathbf{Z}]$) which are non-negative numbers ordered with decreasing amplitude. The unknown coefficients $[\mathbf{I}]$ can be calculated by $[\mathbf{I}] = \sum_{j=1}^{P'} \lambda_j^{-1}[\mathbf{V}_j]([\mathbf{U}_j^H][\mathbf{F}])$ where $[\mathbf{U}_j^H]$ and $[\mathbf{V}_j]$ are the j-th column of $[\mathbf{U}]$ and $[\mathbf{V}]$, which are the left and right singular vectors of $[\mathbf{Z}]$, and the summation is extended to the singular values above a certain error threshold. In Section 6, we will see that having a certain redundancy improves the accuracy of the solution.

It is worth noting that one can also choose as elements of the spectral basis electric and magnetic dipoles orthogonal to the minimum sphere, in place of couples of orthogonal electric dipoles tangential to the minimum sphere, according to an unconventional version of the equivalence theorem presented in [36]. No particular convenience has been found in choosing either tangential electric dipoles or electric and magnetic dipoles orthogonal to the surface.

5. CSP GENERATION BY SPACE SAMPLING AND SPHERICAL WAVE EXPANSION

In this section, an alternative way to generate the CSP expansion is obtained synthesizing the procedure in [33]. Consider again an arbitrary set of sources radiating in free-space. The equivalence principle allows one to replace these sources by equivalent currents distributed over the surface S of the minimum sphere, and providing the same field outside S. In the Love formulation, both electric and magnetic currents are used, whose values are obtained by imposing a null field inside S [37]. An alternative formulation can be provided for equivalent currents of electric type only by imposing inside S an electromagnetic field that guarantees the continuity of the tangential electric field at the interface [38]. Although in general the calculation of these currents requires the solution of a boundary value problem, for the particular case of a spherical equivalence surface, an analytic expression of the equivalent currents can be found after expanding the internal and external electromagnetic field in a set of spherical harmonics and applying mode matching. To this end, consider the expansion of the field radiated outside the equivalence surface S in terms of outgoing spherical wave functions

$$\mathbf{E}(\mathbf{r}) = k\sqrt{\zeta} \sum_{s,m,n} Q_{s,m,n}^{(3)} \mathbf{F}_{s,m,n}^{(3)}(\mathbf{r}) \tag{12}$$

where $\mathbf{r} \equiv (r, \theta, \phi)$ is the observation point, $\mathbf{F}_{s,m,n}^{(3)}$ are spherical wave functions defined as in [39] (except for the opposite convention for time dependence, which is here $\exp(j\omega t)$), and $Q_{s,m,n}^{(3)}$ are the expansion coefficients. The corresponding expression for the equivalent electric currents that radiating alone (i.e., in absence of magnetic current) give the same field as in (12) outside S is

$$\mathbf{J}(r_0\hat{\mathbf{r}}) = \frac{-1}{kr_0^2\sqrt{\zeta}} \sum_{s,m,n} \frac{Q_{s,m,n}^{(3)}}{R_{s,n}^{(1)}(kr_{\min})} \mathbf{T}_{s,m,n}^{(3)}(\hat{\mathbf{r}}) \tag{13}$$

where $r_{\min}$ is the radius of the minimum sphere, $\hat{\mathbf{r}} \equiv (\theta, \phi)$, and the functions $R_{s,n}^{(1)}$ and $\mathbf{T}_{s,m,n}^{(3)}$ result from the factorization $\hat{\mathbf{r}} \times \mathbf{F}_{s,m,n}^{(i)}(\mathbf{r}) = R_{s,n}^{(i)}(kr)\hat{\mathbf{r}} \times \mathbf{T}_{s,m,n}^{(i)}(\hat{\mathbf{r}})$. Equation (13) provides a closed-form expression of the equivalent current distribution which only depends on the coefficients of the spherical wave expansion of the electric field outside S. These coefficients may be directly available from spherical near field measurements, or they can be easily calculated from field samples measured or calculated on a spherical surface external to the minimum sphere. The expression in (13) still holds if the radius of the sphere is analytically continued to a complex value $r_c = r_0 - jb$ with b positive and $r_0 \leq r_{\min}$ arbitrary. With this choice (13) becomes a continuous distribution of CSP source producing directive beam fields radially emerging from the real spherical surface S. Accordingly, the radiation integral over the complex equivalence surface can be interpreted as a continuum of beam contributions

$$\mathbf{E}(\mathbf{r}) = \frac{-1}{k\sqrt{\zeta}} \sum_{s,m,n} \frac{Q_{s,m,n}^{(3)}}{R_{s,n}^{(1)}(k(r_0 - jb))} \iint \underline{\underline{\mathbf{G}}}_{EJ}(\mathbf{r} - \mathbf{r}_c) \cdot \mathbf{T}_{s,m,n}^{(3)}(\hat{\mathbf{r}}) d\Omega \tag{14}$$

where $d\Omega = \sin\theta d\theta d\varphi$, $\underline{\underline{\mathbf{G}}}_{EJ}$ is the electric dyadic Green's function defined in (2), and $\mathbf{r}_c = \hat{\mathbf{r}}(r_0 - jb)$ is the radial vector on the equivalence complex sphere of radius $r_c = r_0 - jb$. The radiation integral in (14) must be properly discretized to yield a finite summation of CSP contributions. Without using any precaution, the number of samples required in this process is very large. In fact, if all the significant terms in (13) are retained, the currents are rapidly varying due to the spherical wave functions with large indexes n and m. However, it is known that the currents associated with higher order spherical wave functions do not significantly contribute to the field radiated at a certain distance from S. As a consequence, when the distance between the source and the observer is larger than a wavelength, the summation over the index n can be truncated to the value $n_{\max} = kr_{\min} + n_1$ without affecting the accuracy of the field representation, n_1 being an integer depending on the position where the field is observed and on the precision required. As a general rule, $n_1 = 1.6(kr_{\min})^{1/3}$ is a satisfactory value for most practical applications [39].

When the surface wave expansion is truncated at $n_{\max}$, a slowly varying equivalent current distribution is obtained; therefore, the radiation integral can be discretized with a DoF- matched number

of angular samples $\hat{\mathbf{r}}_p$ by applying a quadrature rule, yielding

$$\mathbf{E}\left(\mathbf{r}\right) = \sum_{p=1}^{P} \underline{\underline{\mathbf{G}}}_{EJ}\left(\mathbf{r} - \mathbf{r}_p^{(c)}\right) \cdot \left(I_p^{(\theta)}\hat{\boldsymbol{\theta}}_p + I_p^{(\varphi)}\hat{\boldsymbol{\varphi}}_p\right)$$

$$I_p^{\left\{\begin{smallmatrix}\theta\\\varphi\end{smallmatrix}\right\}} = \frac{-w_p}{kr_0^2\sqrt{\zeta}} \sum_{s,m,n<n_{\max}} \frac{Q_{s,m,n}^{(3)}}{R_{s,n}^{(1)}(k\left(r_0 - jb\right))}\mathbf{T}_{s,m,n}^{(3)}\left(\hat{\mathbf{r}}_p\right) \cdot \left\{\begin{smallmatrix}\hat{\boldsymbol{\theta}}_p\\\hat{\boldsymbol{\varphi}}_p\end{smallmatrix}\right.$$

(15)

where $\mathbf{r}_p^{(c)} = (r_0 - jb)\hat{\mathbf{r}}_p$ and w_p are the nodes and the weights of the quadrature scheme, respectively, and $\hat{\boldsymbol{\theta}}_p = \hat{\boldsymbol{\varphi}}_p \times \hat{\mathbf{r}}_p$; $\hat{\boldsymbol{\varphi}}_p = (\hat{\mathbf{z}} \times \hat{\mathbf{r}}_p)/|\hat{\mathbf{z}} \times \hat{\mathbf{r}}_p|$ are the spherical coordinates unit vectors at $r_0\hat{\mathbf{r}}_p$. The notation $n < n_{\max}$ indicates that the summation over index n is truncated to the value $n_{\max} = kr_{\min} + 1.6(kr_{\min})^{1/3}$. The expansion in (15) differs from (10) for a different way to calculate the coefficients, which in (15) are provided directly from the spherical wave expansion, and in (10) by a far field matching. The accuracy of the CSP expansion in (15) only depends on the truncation index chosen for the spherical wave summation and on the quadrature scheme used for the discretization of the radiation integral, which is related to the degrees of freedom.

In order to compare (10) and (15), the space sampling can be done on a space lattice like the one in Figure 1(b), and the number of samples can be determined according to the degrees of freedom. Namely, the space angular sampling is the same for the two procedure; that is $\hat{\mathbf{r}}_p \equiv \hat{\mathbf{k}}_p$. Note that (14) is obtained by analytically extending to complex space the exact expression of the Green's dyad, inclusive of the reactive contributions; for this reason, the CSP fields are exact solution of the wave equation for any value of kb.

As the representation in (10), (15) is extremely efficient when the field is only observed inside a certain angular region, since in that case the angular selectivity of the beams allows one to reduce the number of unknowns needed for the field representation. In both the proposed expansions, the total number of CSP beams is twice the number of nodes used for the discretization of the radiation integrals in (5) and (14). We note that, although the two formulations leading to (10) and (15) are quite different, both approaches are based on an *angular* partition of the integration domain, which is given by the directions $\hat{\mathbf{r}}_p \equiv \hat{\mathbf{k}}_p$. We also note that in the spectral sampling of Section 4, the integration is not carried out directly, because the closed form of the spectral domain CSP is used; thus, the coefficients obtained by the inversion of a linear system require the knowledge of far field samples only. On the other hand, the approach presented in this section requires the knowledge of the coefficients of the spherical wave expansion, whose number approximately matches the degrees of freedom. In both cases, the identification of spatial and spectral samples can be done by using the icosahedral grid method in [35]. This has the advantage of providing a set of beams whose axes are approximately uniformly distributed in the solid angle.

6. COMPARISONS OF THE TWO APPROACHES AND INFLUENCE OF b

In this section, a comparison between the two approaches is given by looking at the error on the reconstruction of a given field for a certain number of CSPs. In general, the accuracy depends on the field to be matched. However, it is known that any field radiated by sources contained inside a given minimum sphere can be accurately represented as a superimposition of spherical harmonics with maximum polar index related to the radius of the minimum sphere. For this reason, useful information can be obtained by considering the error in the reconstruction of spherical harmonics of different orders. In the following, we will use $r_0 = 4\lambda$ and $r_c = r_0(1 - j)$. The relative quadratic error is calculated over a sphere of radius $r = 50\lambda$ as $\varepsilon = \iint_{4\pi} |\mathbf{E}_{ref} - \mathbf{E}_{CSP}|^2 r^2 d\Omega / \iint_{4\pi} |\mathbf{E}_{ref}|^2 r^2 d\Omega$, where $\mathbf{E}_{ref}$ is the field of the spherical wave harmonic of indexes n, $m = n$, $s = 2$. Figure 3 shows the error for different numbers of CSPs as a function of the SW index n. Continuous lines and dashed lines are relevant to spectral and space sampling, respectively. The results have been obtained by using the Lebedev quadrature rule [40] for the lattice and weights generation in the procedure of Section 5. For the sake of consistency, the same lattice has been also used for the procedure described in Section 4. As it can be seen, the method based on space sampling has the same accuracy of the method based on spectral matching as long as
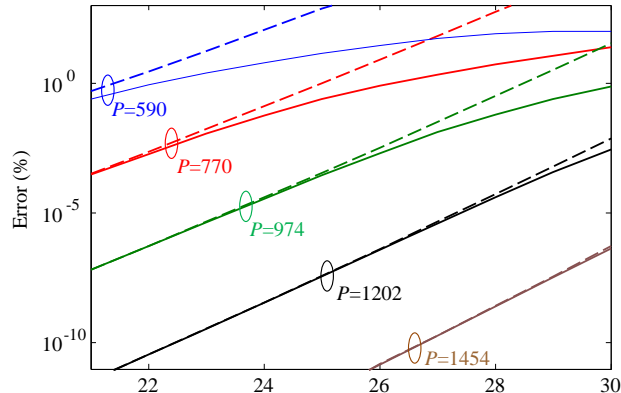
Figure 3. Percent quadratic error in the reconstruction of the field of the SW characterized by the indexes n, $m = n$ and $s = 2$ as a function of the order n and for different numbers of CSPs. Continuous line: spectral matching; dashed line: space sampling of spherical waves.

the number of CSPs is sufficiently high to provide an accurate estimate of the spatial integral. However, when the order of the SW is increased, the accuracy obtained with spectral matching is higher. On the other hand, this method requires the solution of a linear system for the determination of the CSP coefficients, while the other method directly provides them in closed form.

Then, we have analyzed the error as a function of the parameter $b/r_{\min}$, for the two approaches. The optimal value of b is the one requiring the minimum number of beams to obtain a given accuracy, or, equivalently, providing the maximum accuracy for a given number of beams. This value may actually depend on the field to be represented and on the observation region; however, it is possible to provide general guidelines for the choice of this parameter.

For observation in the full angular space, the accuracy of both methods depends slightly on the choice of b and significantly on the redundancy factor η. It is also true that the accuracy depends on the field to be matched. However, the worst reference field $\mathbf{E}_{ref}$ to test the accuracy of the two used procedures is the spherical harmonic of highest order. As mentioned before, this order is given by $n_{\max} \approx kr_{\min} + 1.6(kr_{\min})^{1/3}$. For instance, we will make reference of a minimum sphere of radius $r_{\min} = 4\lambda$, that leads to $n_{\max} \approx 30$ and $N_{DoF} = 1920$, and we will consider the spherical wave harmonic of indexes $n = 30$, $m = n$, $s = 2$. The field is observed at $r = 20\lambda$. Results in Figure 4 compare the errors of the two procedures presented in Sections 4 (spectral matching, continuous line) and 5 (space sampling of SW, dashed lines) as a function of $b/r_{\min}$. Two extreme cases are considered: $r_0 = 0$, corresponding to beams launched from the origin of the reference system (Figure 2(a)), and $r_0 = r_{\min}$, corresponding to beams emerging from the surface of the minimum sphere (Figure 2(b)). Different values of the redundancy factor η defined in (7) have been considered. It is observed that the error is comparable for the two techniques for increasing redundancy and that for small values of b the error is smaller for $r_0 = r_{\min}$. Beams launched from the center have a limit of b from which the expansion starts to have a significant error.

In the method based on spectral sampling, the choice of b also affects the condition number of the system matrix, since small values of b lead to nearly linearly dependent beams. Figure 5 shows the condition number of the system matrix as a function of the beam parameter b for the two cases $r_0 = 0$ and $r_0 = r_{\min}$. Different numbers of spectral samples have been considered for the matching, while the number of beams is kept constant and equal to $2P = 2404$. It is seen that the condition number improve drastically for a small redundancy of samples with respect to the square case $P = Q$, and next stabilizes. For increasing b, the condition number decreases. When the beams are centered at the origin, low values of b imply unacceptable condition number.

From the previous results it is clear that the accuracy is not strongly dependent on the choice of b in the range $b \in [r_{\min}/2, r_{\min}]$. However, this parameter becomes important if the field has to be estimated only in a certain angular region. In fact, in such a case it is preferable to use collimated CSP beams with $b \approx r_{\min}$ or larger. This indeed allows one to exploit the local angular selectivity [41]. This
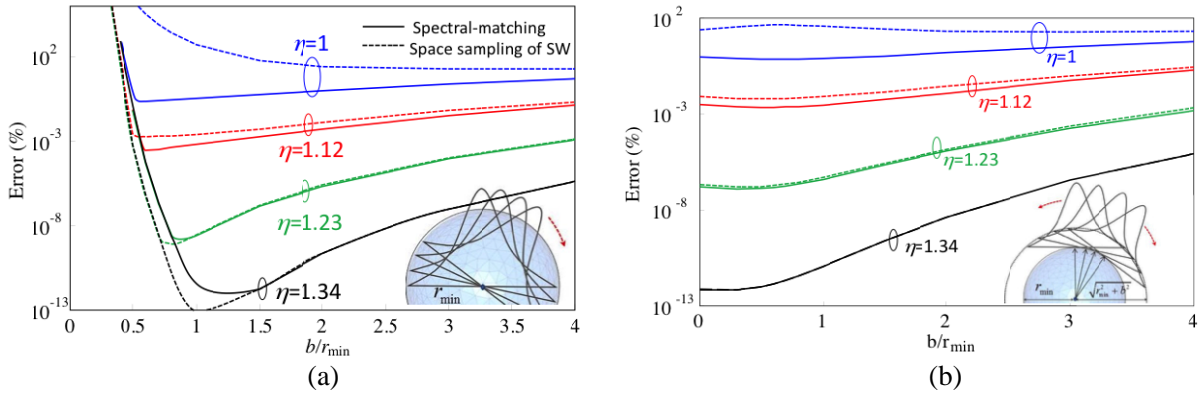
Figure 4. Percent quadratic error of reconstructed field as a function of $b/r_{\min}$ for various values of the redundancy factor η with respect to the degrees of freedom of the field. (a) $r_0 = 0$; (b) $r_0 = r_{\min}$. Continuous line: spectral matching; dashed line: space sampling of spherical waves.
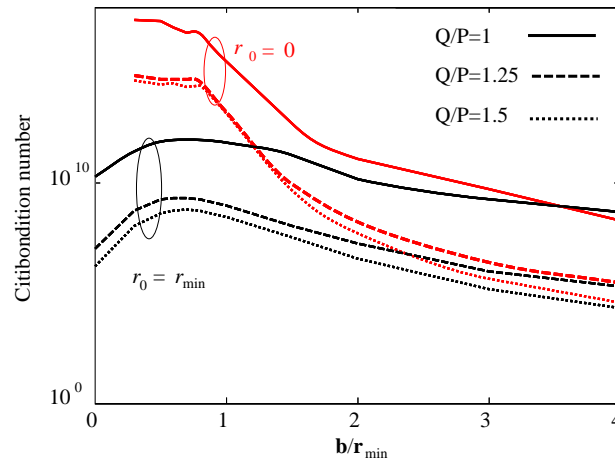
Figure 5. Condition number of the system matrix for spectral sampling as a function of the beam parameter b for the two cases $r_0 = 0$ and $r_0 = r_{\min}$ and various numbers Q of matching points $(2P = 2404)$.

case is of practical importance when dealing with MoM type reaction integrals between groups of basis functions, or in the generalized admittance matrix approach discussed next.

Consider an observation region corresponding to the interior of a cone with apex at the origin, and half-aperture angle α. C_Ω is the angular region associated with this cone, where $\Omega = 2\pi(1 - \cos\alpha)$ denotes the corresponding solid angle. The number N_{DoF}^{Ω} of degrees of freedom of the field inside C_Ω is related to the number N_{DoF} of degrees of freedom associated with the full solid angle by $N_{DoF}^{\Omega} \approx N_{DoF}[\Omega/4\pi]$. The number of CSPs would be reduced by approximately the same factor by retaining in the expansion only those CSP beams whose axis is contained inside the conical region C_Ω. However, due to the finite beamwidth of the beams, this is not sufficient to obtain a good accuracy. It is thus convenient to define a second coaxial "truncation" cone with half-aperture angle $\alpha + \delta$ and to retain in the expansion only the CSP beams whose axis is contained inside this truncation cone. The value of the excess angle δ is chosen so that the amplitude of the field of a CSP beam with axis lying on the boundary of the truncation cone is attenuated of approximately 20 dB at the boundary of C_Ω. For observation distances much larger than b and collimated beams, this condition leads to $\delta \approx 1.5\sqrt{2/kb}$. In such a case the number of beams is equal to $N_{DoF}^{\Omega} \approx N_{DoF}\eta^2[\Omega'/4\pi]$ where $\Omega' = 2\pi(1 - \cos(\alpha + \delta))$ and η is the redundancy factor used.

7. USE OF CSP-BEAMS IN A GENERALIZED ADMITTANCE MATRIX APPROACH

In the generalized scattering matrix approach the analysis domain is decomposed into separate subdomains and the interactions among different subdomains are described through a network formalism where the ports are associated with properly chosen wave objects. To this end, each subdomain is studied with the most appropriate technique and characterized through a generalized scattering matrix (GSM) relating the expansion coefficients of the incident field to those of the reflected field. The main advantages of the GSM approach are: i) the decomposition of the overall problem into simpler sub-problems which are computationally much smaller and parallelizable; ii) the possibility of using the most appropriate technique to solve each sub-problem; iii) the possibility of re-using the GSM as building blocks for a variety of configurations. This characteristic is particularly appealing for problems containing geometrical repetitions and in the context of parametric investigations of complex systems, or antenna siting problems, where several source positions in the same scenario have to be analyzed.

CSP beams radially emerging from the subdomain boundaries can be chosen as wave objects in this GSM scheme [31]. Subdomains containing a source are characterized by the coefficients of the CSP expansion of the radiated field. An m-indexed subdomain containing a scatterer is characterized by a scattering matrix $[\mathbf{S}^{(m)}]$, which is built by illuminating the scatterer with a CSP at a time, calculating the scattered field and projecting the scattered field onto the CSP basis according to the described procedure. This step can be done by considering the object in isolation. The interaction between two sub-domains characterized by $[\mathbf{S}^{(m)}]$ and $[\mathbf{S}^{(n)}]$ is established in closed form on the basis of the so-called generalized transport matrices $[\mathbf{T}^{(m,n)}]$ (Figure 6(a)).

By combining scattering and transport matrices of all the subdomains, a global linear system is obtained. Negligible elements of the transport matrices $[\mathbf{T}^{(m,n)}]$ correspond to couples of non-interacting wave objects, or unconnected ports in the network formalism. A key issue for the efficiency of the process is therefore the sparsification of the transport matrices, namely the minimization of the number of interacting CSP. The previously described CSP expansion allows for reaching this objective in an effective way. In fact, due to their angular selectivity the CSPs match the degrees of freedom also in a limited angular sector, and therefore only a non-redundant number of beams provide a significant contribution in a given region of space.

In addition, CSPs allow for the calculation of the elements of the transport matrices in analytical

(a)

(b)
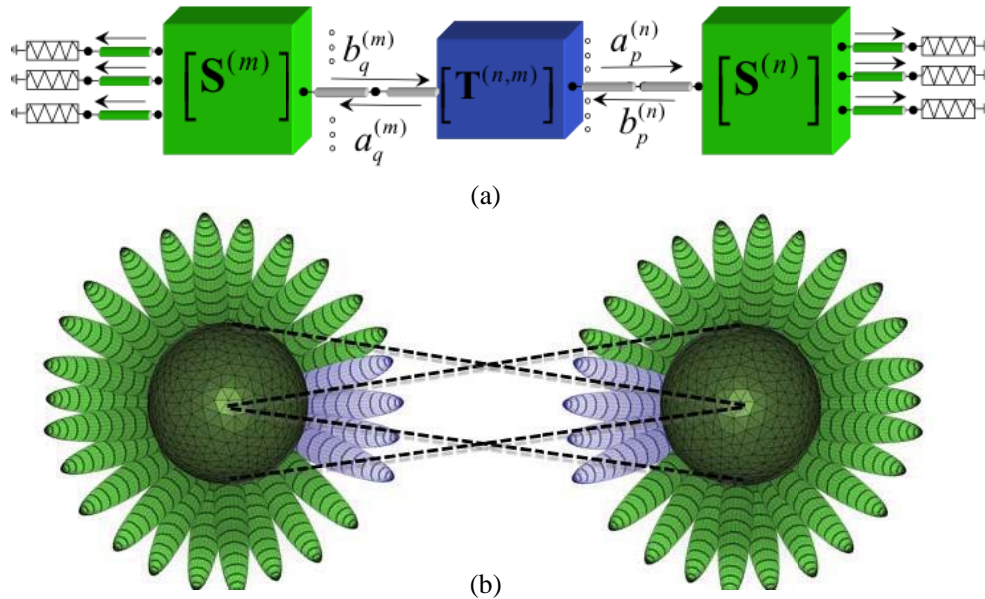
Figure 6. (a) Equivalent network model for the connection of two subdomains through generalized scattering and transport matrices. (b) CSP beams involved in the interaction between two subdomains.

form. In fact, the transport matrix can be calculated on the basis of the impedance matrices of beams $[\mathbf{Z}^{(n,m)}]$ through the relationship $[\mathbf{T}^{(m,n)}] = [\mathbf{Z}^{(n,n)}]^{-1}[\mathbf{Z}^{(n,m)}]$. The entries of the impedance matrices are constituted by the reaction impedances between CSPs. For instance, for two CSPs located at complex points $\mathbf{r}_1^{(c)} = (\mathbf{r}_1 - j\mathbf{b}_1)$ and $\mathbf{r}_2^{(c)} = (\mathbf{r}_2 - j\mathbf{b}_2)$, and oriented along $\hat{\mathbf{u}}_1$ and $\hat{\mathbf{u}}_2$, respectively, the reaction impedance can be calculated as

$$Z^{(1,2)} = \underline{\underline{\mathbf{G}}}_{EJ}(\mathbf{r}_1^{(c)} - \mathbf{r}_2^{(c)}) \cdot \hat{\mathbf{u}}_1 \cdot \hat{\mathbf{u}}_2 \tag{16}$$

which is like sampling the field of the CSP 1 at the location of CSP 2. Thus, the entries of all the transport matrices are in analytical form.

8. CONCLUSIONS

Among the various types of beams, complex source points are extremely easy to be used to expand fields radiated by an arbitrary set of sources in a finite region. Two different generation methods have been presented; in both of them CSP beams emerge from the minimum spherical surface enclosing the real sources, but their weights are calculated using two different processes. In the first process, the spectrum (far field) radiated from the sources is matched to a linear combination of spectral CSPs on a proper spectral lattice by solving a linear system. In the second approach, the coefficients of the linear combination are found in analytical form as a function of the spherical wave expansion coefficients. In both the processes, the number of terms in the CSP expansion almost matches the number of degrees of freedom of the field. The representation has the advantage to satisfy Maxwell's equation from the near to the far region. The resulting representation is particularly efficient when the field knowledge is only required in a limited angular region. These characteristics are important when the field expansion is used for the analysis of the interactions between groups of sources. The latter case can be cast in a network formalism that allows to treat the problem in an extremely efficient way.

The process based on spectral matching and the one using spherical wave expansion provide essentially the same computational performances, leaving to the user the freedom of deciding which is more appropriate on the basis of personal knowledge and available data.

REFERENCES

1. Wylde, R. J., "Millimetre-wave Gaussian beam-mode optics and corrugated feed horns," *IEE Proceedings H, Microwaves, Optics and Antennas*, Vol. 131, No. 4, 258–262, Aug. 1984, Doi: 10.1049/ip-h-1.1984.0053.
2. McEwan, N. J. and P. F. Goldsmith, "Gaussian beam techniques for illuminating reflector antennas," *IEEE Trans. Antennas Propag.*, Vol. 37, No. 3, 297–304, Mar. 1989.
3. Imbriale, W. A. and D. J. Hoppe, "Recent trends in the analysis of quasioptical systems," *Millenium Conf. on Antennas Propag.*, Davos, Switzerland, 2000.
4. Withington, S., J. A. Murphy, and K. G. Isaak, "Representation of mirrors in beam waveguides as inclined phase-transforming surfaces," *Infrared Phys. Technol.*, Vol. 36, No. 3, 723–734, Apr. 1995.
5. Siegman, A., "Hermite-Gaussian functions of complex argument as optical-beam eigenfunctions," *J. Opt. Soc. Am.*, Vol. 63, 1093–1094, 1973.
6. Hernàndez-Figueroa, H. E., M. Zamboni-Rached, and E. Recami (eds.), *Localized Waves*, Chapter 6, Wiley-Interscience, Hoboken, NJ, 2008.
7. Steinberg, B. Z., E. Heyman, and L. B. Felsen, "Phase space methods for radiation from large apertures," *Radio Sci.*, Vol. 26, 219–227, 1991.
8. Shlivinski, A., E. Heyman, A. Boag, and C. Letrou, "A phase-space beam summation formulation for ultrawideband radiation: A multiband scheme," *IEEE Trans. Antennas Propag.*, Vol. 52, No. 8, 2042–2056, Aug. 2004, Doi: 10.1109/TAP.2004.832513.
9. Shlivinski, A., E. Heyman, and A. Boag, "A phase-space beam summation formulation for ultrawideband radiation — Part II: A multiband scheme," *IEEE Trans. Antennas Propag.*, Vol. 53, No. 3, 948–957, Mar. 2005.

10. Shlivinski, A., E. Heyman, and A. Boag, "A pulsed beam summation formulation for short pulse radiation based on windowed radon transform (WRT) frames," *IEEE Trans. Antennas Propag.*, Vol. 53, No. 9, 3030–3048, Sep. 2005.

11. Arnold, J. M., "Phase-space localization and discrete representation of wave fields," *J. Opt. Soc. Am. A*, Vol. 12, No. 1, 111–123, Jan. 1995.

12. Chou, H.-T., P. H. Pathak, and R. J. Burkholder, "Application of Gaussian-ray basis functions for the rapid analysis of electromagnetic radiation from reflector antennas," *IEE Proc. Microw. Antennas Propag.*, Vol. 150, 177–183, 2003.

13. Chou, H.-T. and P. H. Pathak, "Uniform asymptotic solution for electromagnetic reflection and diffraction of an arbitrary Gaussian beam by a smooth surface with an edge," *Radio Sci.*, Vol. 32, No. 4, 1319–1336, Jul./Aug. 1997.

14. Skokic, S., M. Casaletti, S. Maci, and S Sorensen, "Complex conical beams for aperture field representations," *IEEE Trans. Antennas Propag.*, Vol. 50, No. 2, 611–622, Feb. 2011, Doi: 10.1109/TAP.2010.2096379.

15. Sarkar, T. K. and O. Pereira, "Using the matrix pencil method to estimate the parameters of a sum of complex exponentials," *IEEE Antennas and Propagation Magazine*, Vol. 37, No. 1, 48–55, Feb. 1995, Doi: 10.1109/74.370583.

16. Deschamps, G. A., "The Gaussian beam as a bundle of complex rays," *Electron. Lett.*, Vol. 7, No. 23, 684–685, 1971.

17. Felsen, L. B., "Complex-source-point solutions of the field equations and their relation to the propagation and scattering of Gaussian beams," *Proc. Symp. Math.*, Vol. 18, 39–56, 1975.

18. Heyman, E. and L. B. Felsen, "Gaussian beam and pulsed-beam dynamics: Complex-source and complex-spectrum formulations within and beyond paraxial asymptotics," *J. Opt. Soc. Am. A*, Vol. 18, No. 7, 1588–1611, 2001.

19. Yao, D., "Complex source representation of time harmonic radiation from a plane aperture," *IEEE Trans. Antennas Propag.*, Vol. 43, No. 7, 720–723, Jul. 1995.

20. Chow, Y. L., J. J. Yang, D. G. Fang, and G. E. Howard, "A closed form spatial Green function for the microstrip substrate," *IEEE Trans. Microw. Theory Tech.*, Vol. 39, No. 3, 588–592, Mar. 1991.

21. He, J., T. Yu, N. Geng, and L. Carin, "Method of moments analysis of electromagnetic scattering from a general three-dimensional dielectric target embedded in a multilayered medium," *Radio Sci.*, Vol. 35, No. 2, 305–313, 2000.

22. Vipiana, F., A. Polemi, S. Maci, and G. Vecchi, "A mesh-adapted closed-form regular kernel for 3D singular integral equations," *IEEE Trans. Antennas Propag.*, Vol. 56, No. 6, 1687–1698, Jun. 2008.

23. Bucci, O. and G. Franceschetti, "On the degrees of freedom of scattered fields," *IEEE Trans. Antennas Propag.*, Vol. 37, No. 7, 918–926, 1989, Doi: 10.1109/8.29386.

24. Bucci, O., "Computational complexity in the solution of large antenna and scattering problems," *Radio Sci.*, Vol. 40, RS6S16, 2005, Doi: 10.1029/2004RS003196.

25. Stupfel, B. and Y. Morel, "Singular value decomposition of the radiation operator: Application to model-order and far-field reduction," *IEEE Trans. Antennas Propag.*, Vol. 56, No. 6, 1605–1615, 2008, Doi: 10.1109/TAP.2008.923311.

26. Bogush, Jr., A. J. and R. E. Elkins, "Gaussian field expansions for large aperture antennas," *IEEE Trans. Antennas Propag.*, Vol. 34, No. 2, 228–243, 1986.

27. Prakash, V. V. S. and R. Mittra, "Characteristic basis function method: A new technique for efficient solution of method of moments matrix equations," *Microwave Opt. Technol. Lett.*, Vol. 36, No. 2, 95–100, 2003.

28. Matekovits, L., V. Laza, and G. Vecchi, "Analysis of large complex structures with the synthetic-functions approach," *IEEE Trans. Antennas Propag.*, Vol. 55, No. 9, 2509–2521, 2007, Doi: 10.1109/TAP.2007.90407.

29. Casaletti, M., S. Maci, and G. Vecchi, "Diffraction-like synthetic functions to treat the scattering from large polyhedral metallic object," *Appl. Comput. Electromagn. Soc.*, Vol. 24, No. 2, 161–173, 2009.

30. Tap, K., P. H. Pathak, and R. J. Burkholder, "Exact complex source point beam expansions for electromagnetic fields," *IEEE Trans. Antennas Propag.*, Vol. 59, No. 9, 3379–3390, 2011, Doi: 10.1109/TAP.2011.2161438.

31. Martini, E., G. Carli, and S. Maci, "A domain decomposition method based on a generalized scattering matrix formalism and a complex source expansion," *Progress In Electromagnetics Research B*, Vol. 19, 445–473, 2010.

32. Norris, A. N. and T. B. Hansen, "Exact complex source representations of time-harmonic radiation," *Wave Motion*, Vol. 25, 127–141, 1997.

33. Martini, E. and S. Maci, "A closed-form conversion from spherical-wave- to complex-point-source-expansion" *Radio Sci.*, Vol. 46, RS0E22, 2011, Doi: 10.1029/2011RS004665.

34. Devaney, A. J. and E. Wolf, "Radiating and nonradiating classical current distributions and the fields they generate," *Phys. Rev. D*, Vol. 8, 1044–1047, 1973.

35. Sadourny, R., A. Arakawa, and Y. Mintz, "Integration of the nondivergent barotropic vorticity equation with an icosahedral-hexagonal grid for the sphere," *Mon. Wea. Rev.*, Vol. 96, 351–356, 1968, Doi: http://dx.doi.org/10.1175/1520-0493(1968)096<0351:IOTNBV>2.0.CO;2.

36. Rumsey, V. H., "Some new forms of Huygens' principle," *IRE Transactions on Antennas and Propagation*, Vol. 7, No. 5, 103–116, Dec. 1959, Doi: 10.1109/TAP.1959.1144766.

37. Harrington, R. F., *Time Harmonic Electromagnetics*, McGraw-Hill, New York, 1961.

38. Martini, E., G. Carli, and S. Maci, "An equivalence theorem based on the use of electric currents radiating in free space," *IEEE Antennas Wireless Propag. Lett.*, Vol. 7, 421–424, 2008, Doi: 10.1109/LAWP.2008.2001764.

39. Hansen, J. E., *Spherical Near-field Antenna Measurements*, Peter Peregrinus, London, 1988.

40. Lebedev, V. I., "A quadrature formula for the sphere of the 131st algebraic order of accuracy," *Dokl. Math.*, Vol. 59, No. 3, 477–481, 1999.

41. Heilpern, T., E. Heyman, and V. Timchenko, "A beam summation algorithm for wave radiation and guidance in stratified media," *J. Acoust. Soc. Am.*, Vol. 121, No. 4, 1856–1864, 2007, Doi: 10.1121/1.2537221.